A convolutional neural network for intracranial hemorrhage detection in non-contrast CT

Ajay Patel, Rashindra Manniesing

Ajay Patel, Rashindra Manniesing, "A convolutional neural network for intracranial hemorrhage detection in non-contrast CT," Proc. SPIE 10575, Medical Imaging 2018: Computer-Aided Diagnosis, 105751B (27 February 2018); doi: 10.1117/12.2292975

Event: SPIE Medical Imaging, 2018, Houston, Texas, United States

A Convolutional Neural Network for Intracranial Hemorrhage Detection in Non-Contrast CT

Ajay Patel and Rashindra Manniesing

Diagnostic Image Analysis Group
Department of Radiology and Nuclear Medicine
Radboud University Medical Center, Nijmegen, the Netherlands

ABSTRACT

The assessment of the presence of intracranial hemorrhage is a crucial step in the work-up of patients requiring emergency care. Fast and accurate detection of intracranial hemorrhage can aid treating physicians by not only expediting and guiding diagnosis, but also supporting choices for secondary imaging, treatment and intervention. However, the automatic detection of intracranial hemorrhage is complicated by the variation in appearance on non-contrast CT images as a result of differences in etiology and location. We propose a method using a convolutional neural network (CNN) for the automatic detection of intracranial hemorrhage. The method is trained on a dataset comprised of cerebral CT studies for which the presence of hemorrhage has been labeled for each axial slice. A separate test dataset of 20 images is used for quantitative evaluation and shows a sensitivity of 0.87, specificity of 0.97 and accuracy of 0.95. The average processing time for a single three-dimensional (3D) CT volume was 2.7 seconds. The proposed method is capable of fast and automated detection of intracranial hemorrhages in non-contrast CT without being limited to a specific subtype of pathology.

Keywords: Intracranial hemorrhage, computed tomography, CT, convolutional neural network, CNN

1. INTRODUCTION

Intracranial hemorrhage is a deadly condition that can have debilitating consequences for survivors. Hemorrhages within the cranial vault and surrounding meningeal spaces may among others be caused by traumatic injury, stroke and underlying pathology, such as tumors and vascular malformations.[1] Neuroimaging plays a crucial role for treating physicians, with CT being the most commonly used modality due to its speed and widespread availability in an emergency setting.[2] The timely detection and localization of intracranial hemorrhage is essential for diagnosis, treatment planning and intervention.[3] The assessment of the presence of hemorrhage is the fundamental step in the work-up of acute stroke, as the administration of clot-dissolving thrombolytic drugs can have disastrous consequences in actively bleeding patients.

The appearance of intracranial hemorrhages varies depending on their anatomical origin, location and cause. Hemorrhages may demonstrate variations of size, irregularity, heterogeneity and diffusion within the cranial cavity. In total five subtypes of intracranial hemorrhage can be identified: intracerebral, intraventricular, epidural, subdural and subarachnoid as shown in Figure 1. Also, factors such as image noise, signal attenuation and artifacts may negatively influence their appearance on CT. Automatic detection of such, sometimes very subtle, pathology may contribute to faster diagnosis and treatment, leading to improved patient outcome.[4]

Related work has described methods for the automatic segmentation and volumetric analysis of different intracranial hemorrhage subtypes.[5–7] However, as of yet no method dedicated to the fast detection of intracranial hemorrhage in general exists.

Send correspondence to: Ajay.Patel@radboudumc.nl

Medical Imaging 2018: Computer-Aided Diagnosis, edited by Nicholas Petrick, Kensaku Mori, Proc. of SPIE Vol. 10575, 105751B · © 2018 SPIE · CCC code: 1605-7422/18/$18 · doi: 10.1117/12.2292975

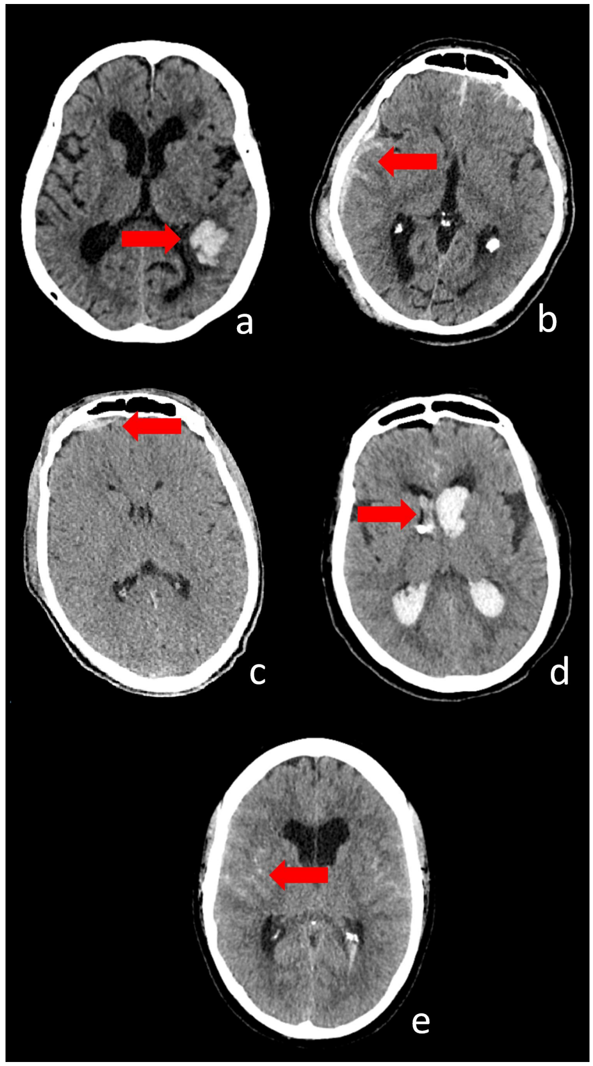

Figure 1. Examples of different intracranial hemorrhage subtypes indicated by red arrows. Intracerebral hemorrhage (a), subdural hemorrhage (b), epidural hemorrhage (c), intraventricular hemorrhage (d) and subarachnoid hemorrhage (e).

In recent years, the interest in the use of convolutional neural networks (CNN) for automated image analysis purposes has shown a rapid increase. CNNs have proven to be capable of producing outstanding results for image recognition and classification tasks in computer vision.[8–10] Furthermore, CNNs are not only able to distinguish between a multitude of labels for image classification, they can do so with speed and accuracy that surpass human performance.[11, 12] Therefore, the implementation of CNNs for medical image analysis may have a powerful impact on detection and classification tasks in emergency situations where these factors are of utmost importance.

In this paper, we propose a method employing a CNN for the fast and automatic detection of intracranial hemorrhage in non-contrast CT. The method is evaluated by comparison to a manually labeled reference standard.

2. METHOD

2.1 Data

This study was approved by the institutional ethics committee, and the requirement for informed consent was waived. Anonymized data was obtained from our clinical image database by retrospectively searching for patients that had received a non-contrast CT in the period January 2015 - December 2015. Patients were included in the positive dataset if the presence of an intracranial hemorrhage was confirmed in the radiologist's report. Patients not demonstrating hemorrhage or other pathology were included in the negative dataset. Further exclusion criteria were the presence of severe motion artifacts or implanted foreign objects, such as clips, drains and coils. All images were acquired using a 320-row Toshiba Acquilion ONE CT scanner manufactured by Toshiba Medical Systems Corporation, Otawara, Japan. The average image size was 512 x 512 x 320 voxels with voxel sizes of 0.43 x 0.43 x 0.5 mm. All cases were labeled by a trained observer to indicate the presence or absence of intracranial hemorrhage for each axial slice.

The total dataset consisted of 95 positive and 95 negative patients, consisting of 13433 positive and 45906 negative labeled 2D axial slices. These were separated into training, validation and test sets as described in Table 1.

Table 1. Overview of study data. Number of positive and negative patients and labeled 2D axial slices for training, validation and test sets.

	Patients		Slices	
	Positive	Negative	Positive	Negative
Training	75	75	10831	35490
Validation	10	10	1258	5378
Test	10	10	1344	5038
Total	95	95	13433	45906

2.2 Network architecture

A two-dimensional (2D) CNN inspired by recent work is proposed.[13] The CNN makes use of the full image context for the prediction of the presence of intracranial hemorrhage, as shown in Figure 2.

The input for the CNN consists of a 512 x 512 voxels image. The architecture consists of five repetitions of a combination of two convolutions of 3 x 3 followed by a rectified linear unit (ReLu) and subsequent max pooling of 2 x 2 with strides of two in each direction. The number of filters is doubled after each max pooling operation. The final feature maps pass through two fully connected layers. Batch normalization (BN) is used for each convolution to normalize the layer's inputs.[14] A softmax function is finally calculated to obtain the probability of the presence of intracranial hemorrhage in the input image.

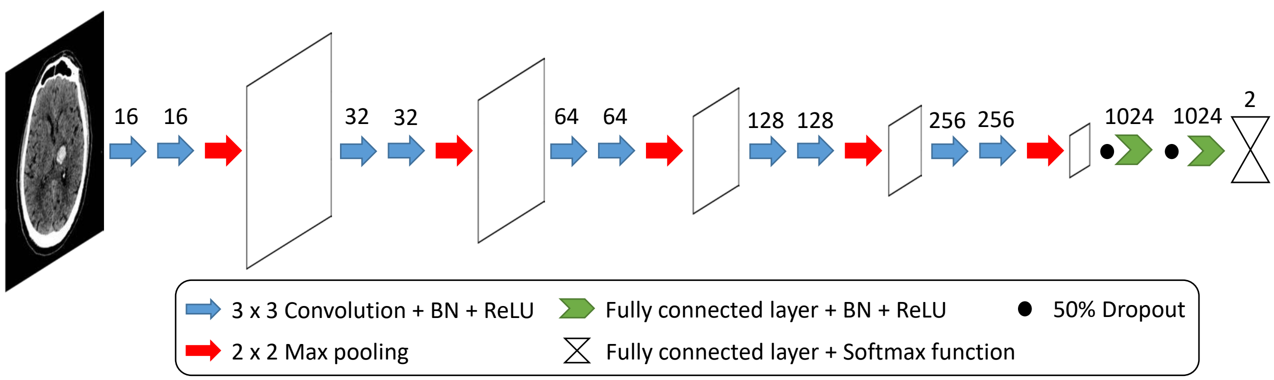

Figure 2. Schematic overview of convolutional neural network architecture. Squares represent feature maps at different depths. The numbers above arrows represent the number of filters applied. ReLu denotes a rectified linear unit. Batch normalization (BN) is used for each convolution to normalize the layer's inputs.

2.3 Training

For each CT study the cranial cavity is segmented using multi-atlas registration and levelset refinement.[15] An equal number of positive and negative training samples are presented to the CNN during training. Axial slices are randomly extracted with equal probability from all patients in the positive and negative training datasets, where the selection is limited to slices depicting part of the cranial cavity. Adam optimization is used to minimize the cross-entropy loss function with an initial learning rate of 0.001. Dropout of 50% is used before and after the first fully connected layer for regularization, as shown in Figure 2. Data augmentation consisting of random rotations within a range of (-15, 15) degrees, random shifts within a range of (-10, 10) voxels in both directions and mirroring on the horizontal axis were used to enrich the training data. The network was trained for 1000 iterations of 500 samples in batches of 25 axial slices on an NVIDIA GeForce GTX 1080 GPU. The method was developed using the Theano and Lasagne libraries.[16,17]

3. RESULTS

Sensitivity, specificity and accuracy were used as quantitative measures to evaluate the performance of the CNN. All measures were calculated in comparison to the reference standard. All axial slices depicting part of the cranial cavity were processed for each test case. True positives, true negatives, false positives and false negatives were counted and the quantitative measures were calculated over the entire test dataset. The results are shown in Table 2. Quantitative evaluation shows a high degree of accuracy, with a value of 0.95 for the entire test dataset. The average processing time for a single 3D CT volume was 2.7 seconds.

Table 2. Overview of quantitative evaluation results. Sensitivity, specificity and accuracy reported for the negative and positive test sets and entire dataset.

	Sensitivity	Specificity	Accuracy
Positive	0.87	0.92	0.91
Negative		1.00	1.00
Full Dataset	0.87	0.97	0.95

The variation in appearance of intracranial hemorrhages and healthy cerebral parenchyma caused the method to produce several false positive and false negative predictions. Examples of axial slices that the method had difficulty with and resulted in such false predictions can be seen in Figure 3 and Figure 4.

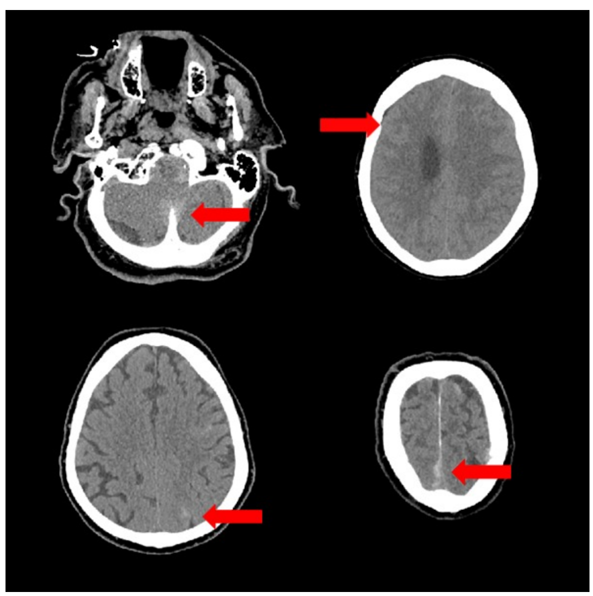

Figure 3. Examples of axial slices that resulted in false positive predictions. Errors are most likely caused by the presence of high intensity regions in the cerebral parenchyma (red arrows).

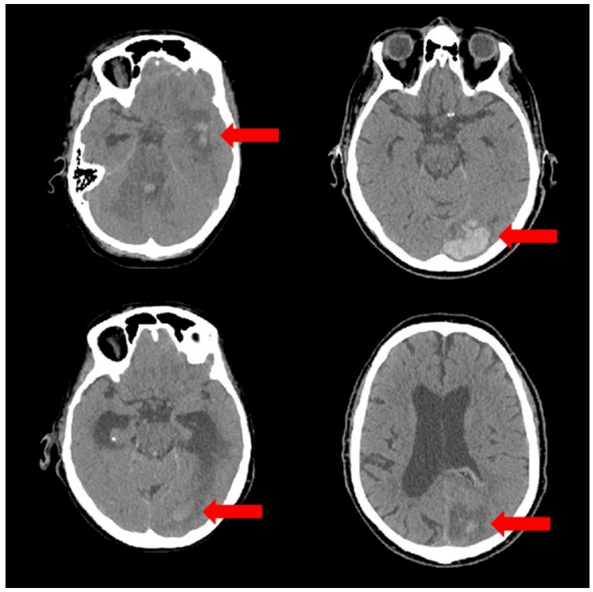

Figure 4. Examples of axial slices that resulted in false negative predictions. The presence of intracranial hemorrhage is missed by the method (red arrows).

4. DISCUSSION

We present a 2D CNN for the automatic detection of intracranial hemorrhages in non-contrast 3D CT. This approach provides enormous speed and a high level of accuracy for a task that necessitates both. We demonstrate that the proposed method shows promising results without being limited to a specific subtype of pathology.

5. CONCLUSION

The described CNN architecture has shown to produce good results in comparison to the reference standard. Accurate and fast detection of intracranial hemorrhage is essential in the work-up of emergency room patients and may aid physicians in diagnosis and guide decisions for treatment and intervention.

ACKNOWLEDGMENTS

This work was supported by research grants from the Dutch Technology Foundation, (STW), the Netherlands, 13350 and Toshiba Medical Systems Corporation, Japan.

REFERENCES

[1] Freeman, W. D. and Aguilar, M. I., "Intracranial hemorrhage: diagnosis and management," *Neurologic Clinics* **30**(1), 211–240 (2012).

[2] Hemphill III, J., Greenberg, S., Anderson, C., Becker, K., Bendok, B., Cushman, M., et al., "American Heart Association Stroke Council; Council on Cardiovascular and Stroke Nursing; Council on Clinical Cardiology. Guidelines for the management of spontaneous intracerebral hemorrhage: a guideline for healthcare professionals from the American Heart Association/American Stroke Association," *Stroke* **46**(7), 2032–2060 (2015).

[3] Heit, J. J., Iv, M., and Wintermark, M., "Imaging of intracranial hemorrhage," *Journal of Stroke* **19**(1), 11–27 (2017).

[4] Vermeulen, M. J. and Schull, M. J., "Missed diagnosis of subarachnoid hemorrhage in the emergency department," *Stroke* **38**(4), 1216–1221 (2007).

[5] Boers, A., Zijlstra, I., Gathier, C., van den Berg, R., Slump, C. H., Marquering, H., and Majoie, C., "Automatic quantification of subarachnoid hemorrhage on noncontrast CT," *American Journal of Neuroradiology* **35**(12), 2279–2286 (2014).

[6] Muschelli, J., Sweeney, E. M., Ullman, N. L., Vespa, P., Hanley, D. F., and Crainiceanu, C. M., "PItcH-PERFeCT: Primary Intracranial Hemorrhage Probability Estimation using Random Forests on CT," *NeuroImage: Clinical* **14**, 379–390 (2017).

[7] Scherer, M., Cordes, J., Younsi, A., Sahin, Y.-A., Götz, M., Möhlenbruch, M., Stock, C., Bösel, J., Unterberg, A., Maier-Hein, K., et al., "Development and validation of an automatic segmentation algorithm for quantification of intracerebral hemorrhage," *Stroke* **47**(11), 2776–2782 (2016).

[8] He, K., Zhang, X., Ren, S., and Sun, J., "Deep residual learning for image recognition," in [*Proceedings of the IEEE Conference on Computer Vision and Pattern Recognition*], 770–778 (2016).

[9] Szegedy, C., Liu, W., Jia, Y., Sermanet, P., Reed, S., Anguelov, D., Erhan, D., Vanhoucke, V., and Rabinovich, A., "Going deeper with convolutions," in [*Proceedings of the IEEE Conference on Computer Vision and Vattern Recognition*], 1–9 (2015).

[10] Krizhevsky, A., Sutskever, I., and Hinton, G. E., "Imagenet classification with deep convolutional neural networks," in [*Advances in Neural Information Processing Systems*], 1097–1105 (2012).

[11] Gulshan, V., Peng, L., Coram, M., Stumpe, M. C., Wu, D., Narayanaswamy, A., Venugopalan, S., Widner, K., Madams, T., Cuadros, J., et al., "Development and validation of a deep learning algorithm for detection of diabetic retinopathy in retinal fundus photographs," *JAMA* **316**(22), 2402–2410 (2016).

[12] Esteva, A., Kuprel, B., Novoa, R. A., Ko, J., Swetter, S. M., Blau, H. M., and Thrun, S., "Dermatologist-level classification of skin cancer with deep neural networks," *Nature* **542**(7639), 115–118 (2017).

[13] Simonyan, K. and Zisserman, A., "Very deep convolutional networks for large-scale image recognition," *arXiv preprint arXiv:1409.1556* (2014).

[14] Ioffe, S. and Szegedy, C., "Batch normalization: Accelerating deep network training by reducing internal covariate shift," in [*International Conference on Machine Learning*], 448–456 (2015).

[15] Patel, A., van Ginneken, B., Meijer, F. J., van Dijk, E. J., Prokop, M., and Manniesing, R., "Robust cranial cavity segmentation in CT and CT perfusion images of trauma and suspected stroke patients," *Medical Image Analysis* **36**, 216–228 (2017).

[16] The Theano Development Team, Al-Rfou, R., Alain, G., Almahairi, A., Angermueller, C., Bahdanau, D., Ballas, N., Bastien, F., Bayer, J., Belikov, A., et al., "Theano: A Python framework for fast computation of mathematical expressions," *arXiv preprint arXiv:1605.02688* (2016).

[17] Dieleman, S., Schlter, J., Raffel, C., Olson, E., Snderby, S. K., Nouri, D., Maturana, D., Thoma, M., Battenberg, E., Kelly, J., Fauw, J. D., Heilman, M., de Almeida, D. M., McFee, B., Weideman, H., Takcs, G., de Rivaz, P., Crall, J., Sanders, G., Rasul, K., Liu, C., French, G., and Degrave, J., "Lasagne: First release.," (Aug. 2015).